Headline Articles

Surface-Enhanced Raman Imaging (SERI) of Patterned Self-Assembled Monolayers of Various Derivatized Thiophenols on Silver

Donald A. Tryk, Xiaomin Yang, Kazuhito Hashimoto, and Akira Fujishima*

Department of Applied Chemistry, Faculty of Engineering, The University of Tokyo, 7-3-1 Hongo, Bunkyo-ku, Tokyo 113

(Received July 7, 1997)

Surface-enhanced Raman imaging (SERI) has recently been developed in our laboratory as an imaging technique which is chemically selective, has monolayer sensitivity, and can be used under ambient conditions. A particularly interesting application of this technique is to image patterned self-assembled monolayers (SAMs). In the present work, we have used both photopatterning and microcontact printing techniques for preparing patterned SAMs with several different terminal functional groups (NO_2, OH, COOH, and CH_3) on evaporated silver films and have imaged them using SERI. The intrinsic subsurface roughness of the film provides sufficient enhancement for the imaging.

The development of chemically selective surface imaging techniques for molecular monolayers has received much attention.[1—22] Such techniques have been used principally to examine micrometer-scale patterns produced in either Langmuir–Blodgett films or self-assembled monolayers (SAMs). For example, secondary ion mass spectroscopic (SIMS) microscopy has been used extensively.[1—5] Other techniques which have been used include optical microscopy (combined with condensation of liquid droplets),[6—13] fluorescence microscopy,[14—16] scanning force microscopy and related techniques,[17—20] and scanning electron microscopy (SEM).[3,9—11,21,22]

In recent years, surface-enhanced Raman scattering (SERS) has developed into a powerful spectroscopic technique because of its combination of sensitivity and rich chemical information content. It has been applied more frequently to the characterization of SAMs as more highly sensitive instrumentation has become available.[23—36] At the same time, micro-Raman imaging has emerged as a powerful technique.[30,37—46] Because Raman peaks are often quite narrow, they are ideal as a means of producing chemically meaningful image contrast. In addition, Raman in general is highly versatile, being usable in a variety of types of environments, as long as the surface or interface is accessible to visible light. Thus the combination of the SERS technique with micro-Raman imaging offers high sensitivity together with spatially resolved chemical information and versatility. Evans et al. were the first to report the combined use of SERS and Raman imaging in examining a self-assembled monolayer on a roughened gold surface,[30] and we have continued to develop this technique, which we have termed surface-enhanced Raman imaging (SERI).[47—51]

Examples of the applications of the SERI technique include the following: examination of the morphology of an electrochemically roughened silver surface, using adsorbed pyridine as a probe molecule;[47] imaging of a pattern produced in a SAM via UV illumination through a photomask;[48] imaging of a patterned monolayer produced by microcontact printing;[49] examination of the surface structure dependence of a photochemical reaction occurring on roughened silver;[50] and observation of the effect of laser illumination on the silver morphology of roughened silver during oxidation–reduction cycles (ORC).[51] In this paper, we describe the SERI technique and focus in greater detail on the use of SERI for imaging molecular monolayers which have been patterned using either 1) UV illumination through a photomask or 2) microcontact printing.

One of the most important aspects of the present work is the fact that SERS can be used effectively in the examination of molecular monolayers on relatively smooth silver surfaces. It has long been recognized that SER spectra can be obtained on evaporated silver or gold surfaces with either very little roughness or at most with subsurface roughness on the order of 50—100 nm,[32,52—57] and it has also recently been demonstrated that even surfaces with a high degree of perfection such as Au(111)/mica can be used.[28,29] In the present work, the use of evaporated silver films with some degree of intrinsic roughness was considered to be a reasonable compromise. On one hand, it was desired to examine SAMs on relatively flat surfaces; on the other hand, however, in

order to obtain spatially resolved chemical information, but not necessarily orientational information, it was considered unnecessary to use surfaces with atomic-level flatness.

The aromatic nitro-compound *p*-nitrothiophenol (PNTP) was used as a Raman probe in the photopatterning experiments. Aromatic nitro compounds are known to be photochemically reactive, with the possible photoproducts including aromatic amines and azobenzene.[34,58—62]

The microcontact printing technique, which has been developed intensively by the Whitesides group,[9—11,20,63—66] is convenient for preparing patterned SAMs. We have used this technique in the present work to prepare several different types of SAMs, both from PNTP and from thiophenols with three other types of para-substituents: OH, COOH, and CH_3.

The SERI technique is expected to have a number of interesting applications in terms of imaging molecular monolayers, and these will be discussed briefly.

Experimental

Sample Preparation and Photopatterning. *p*-Nitrothiophenol (PNTP, 99%) was purchased from Tokyo Kasei Co. and used as received. Absolute ethanol was used to prepare 1—5 mM PNTP solutions (1 M = 1 mol dm^{-3}). Silver films approximately 200 nm thick were freshly evaporated onto ultrasonically cleaned ITO glass (Asahi Glass Co., Ltd.). The films were immersed in the PNTP solutions for at least 24 h in order to allow the SAMs to form. The films were then rinsed with ethanol and dried under a stream of dry Ar. UV illumination was provided by a Hg–Xe lamp (Model LA-200UV, Hayashi Co., Ltd.). Since the UV absorption peak for PNTP is at approximately 320 nm, a 313 nm filter was used. The UV light was focused uniformly on the sample with a power density of 30 mW cm^{-2}. For patterning, a Cu grid (40 lines per mm, 3 mm diameter, Oken Co., Ltd.) was placed directly on the PNTP SAM on Ag for approximately 30 min during the illumination in ambient air.

Microcontact Printing. A lithographic mask (Cr pattern on glass substrate, with a line width of 7 μm, a gap between lines of 7 μm, and a Cr film thickness of 0.5 μm, supplied by the Oken Co., Ltd.) was used as a stamp. However, it should be noted that the type of elastomeric stamp used by the Whitesides group is more suitable because it can make better mechanical contact with the surface of the metal film on glass even if the two surfaces are not extremely flat; since it is absorbent, it can also act as an ink reservoir.[9—11,20,63—66] Solutions (1—5 mM) of *p*-nitrothiophenol (PNTP, 99%, Tokyo Kasei Co., Ltd.) in absolute ethanol were used as the "ink", which was first absorbed into a piece of filter paper; then the Cr-patterned glass was touched to the paper. After inking, the stamp was placed gently on the 200-nm silver thin film, which had been freshly evaporated onto ultrasonically cleaned ITO glass (Asahi Glass Co., Ltd.). Then, hand pressure was applied for ca. 30 min to ensure contact between the stamp and the silver surface. After imprinting, the sample surface was rinsed with ethanol and dried under a stream of Ar. For the preparation of patterned silver surfaces with *p*-hydroxythiophenol, *p*-carboxythiophenol, and *p*-methylthiophenol (Tokyo Kasei Kogyo Co., Ltd.), the same procedure as that for p-nitrothiophenol was followed. The SERS spectra and images were then immediately recorded in ambient air.

Raman Measurements. The SERS spectra and images were recorded in ambient air with a Renishaw System 2000 imaging microscope (Renishaw Co., UK), which has been modified for collection of Raman images in a computer-controlled, point-by-point mode, as described in previous publications from this laboratory (Fig. 1).[39,41,42,47—49] This system uses a single monochromator together with a Raman holographic filter, so that the throughput is much higher than in conventional Raman systems. This system has the capability of obtaining full spectra in less than 1 s. The 514.5 nm Ar^+ laser line was used as the excitation source. The laser light was focused onto the sample using a 50× objective lens mounted on an Olympus BH-2 microscope, with a spot size of approximately 1—2 μm. The SERS imaging was performed with approximately 50 μW laser power at the sample. The sample was placed below the objective lens on an XYZ stage (Newport M-462–XYZ-M) equipped with stepper motors (Newport 850B), which were controlled by a motion controller (Newport PMC400). The sample surface was scanned sequentially in 1 μm steps, and full spectra (780—1640 cm^{-1}) were obtained in approximately 0.6 s at each point. Integrated Raman intensities at each point in the 2D image were obtained by integrating the intensities over a 10 cm^{-1} range on either side of the wavenumber of interest. The acquisition time for a full image was typically 30—40 min. All of the SERS images were background-corrected by subtracting an image obtained in an off-peak portion of the spectrum close to the peak of interest.

AFM Measurements. The atomic force microscopy (AFM) measurements was performed in the contact mode with a Seiko SPA-300 system. A triangular cantilever with integral pyramidal Si_3N_4 tip was used. The typical imaging force was on the order of 10^{-9} N.

Results and Discussion

AFM Characterization of Evaporated Silver Films. As pointed out by Caldwell et al.,[29] work devoted to the characterization of SAMs with SERS has lagged behind that carried out with infrared spectroscopy due to the common perception that SERS requires substantial roughening of Ag and Au surfaces, which is incompatible with the preparation of well ordered, well defined SAMs. However, as already stated, if orientational information is not needed, some degree of roughness can be tolerated, particularly, as in the present work, if the signal-to-noise ratio must be maximized. This requirement is dictated by the fact that full spectra are

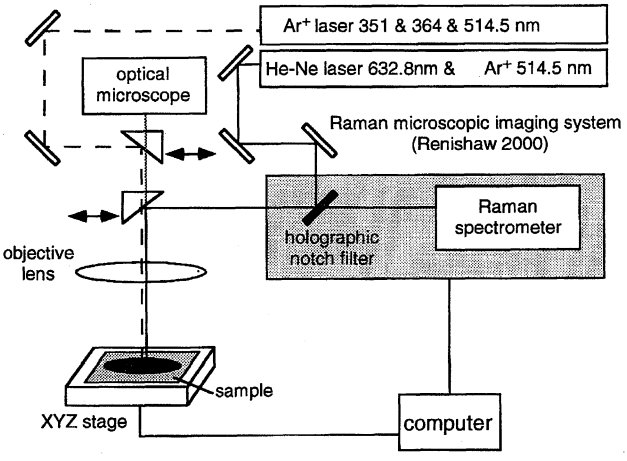

Fig. 1. Experimental set-up for surface-enhanced Raman imaging.

being acquired in a point-by-point imaging mode.

The macroscopically smooth, mirror-like surface is often characterized by subsurface roughness, with particles in the range of 50—100 nm in diameter (Fig. 2). This type of roughness, however, is well known to produce Raman enhancement factors on the order of 10^4,[55,57] consistent with very recent theoretical predictions which are based on the electromagnetic enhancement mechanism and which explicitly include interparticle effects.[67] Thus, not only is it possible to carry out spectroscopic characterization, but it is possible to use surface-enhanced Raman in a two-dimensional imaging mode.

SERS Imaging of Photopatterned SAMs. The formation of patterned monolayers typically involves the two-dimensional control of the placement of SAMs with two or more different terminal groups. One method for producing such patterns makes use of UV illumination, which can cause substantial chemical modifications, leading to changes in the Raman spectra.[3—6,13,68] The principle of photopatterning is shown diagramatically in Fig. 3. We have recently demonstrated that it is possible to image a photopatterned PNTP-based SAM using SERI, with a resolution of ca. 2 μm, without roughening the silver surface.[48]

Evidence for the assembly of a monolayer on the silver surface was the loss of the characteristic S–H stretching band at 2550 cm^{-1} (Fig. 4).[23,24,26] The Raman peaks in the as-assembled layer are found at 855, 1080, 1335, and 1571 cm^{-1} (Fig. 5, curve b), which correspond closely to those in the PNTP powder spectrum (Fig. 5, curve a; see also Table 1).[33] This observation is noteworthy only because there are a number of instances in which SERS spectra are reported for either PNTP or PNBA (*p*-nitrobenzoic acid) which are

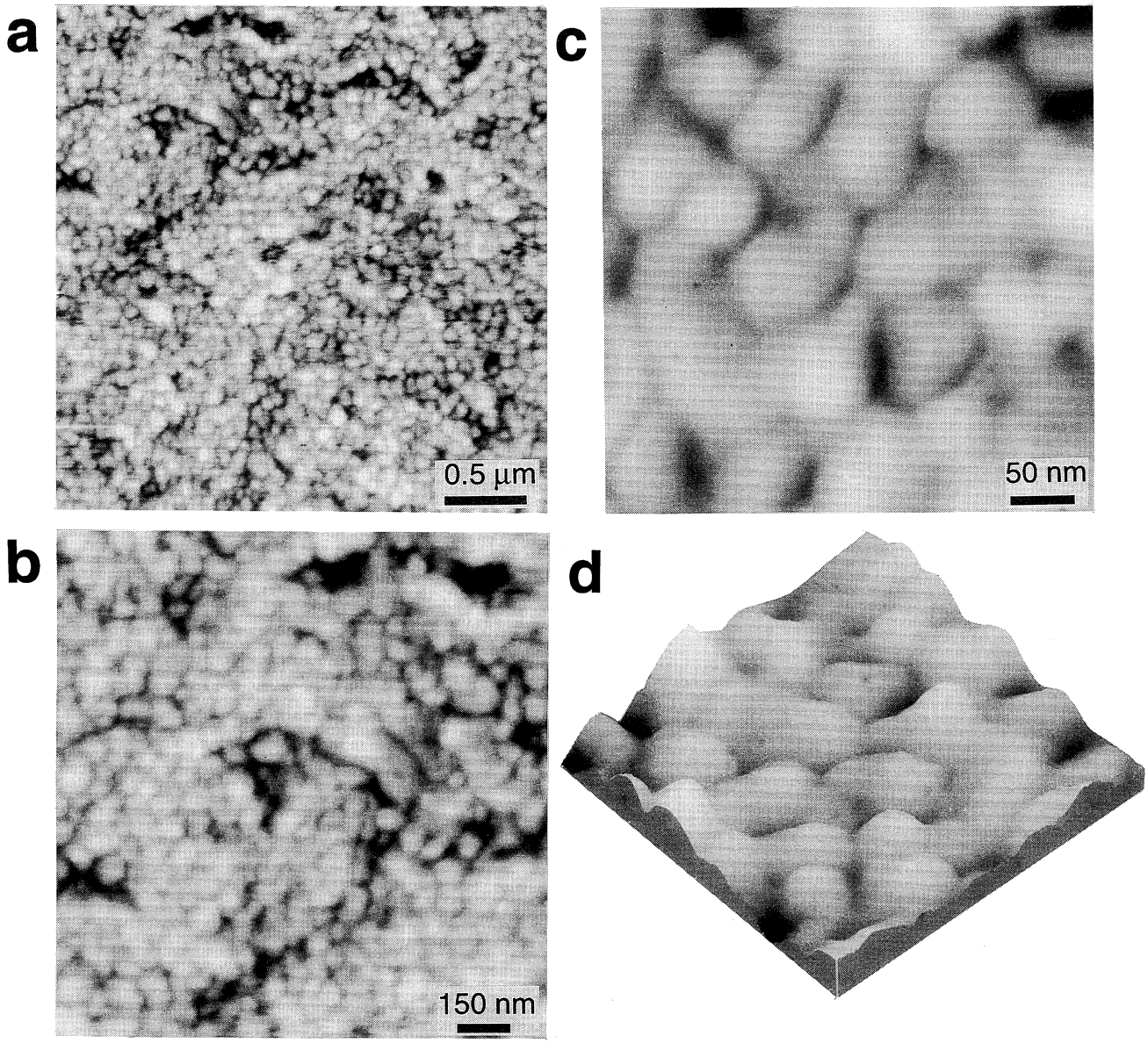

Fig. 2. AFM images of the evaporated silver surface at a) low resolution, b) medium resolution, c) high resolution, and d) 3D representation at high resolution.

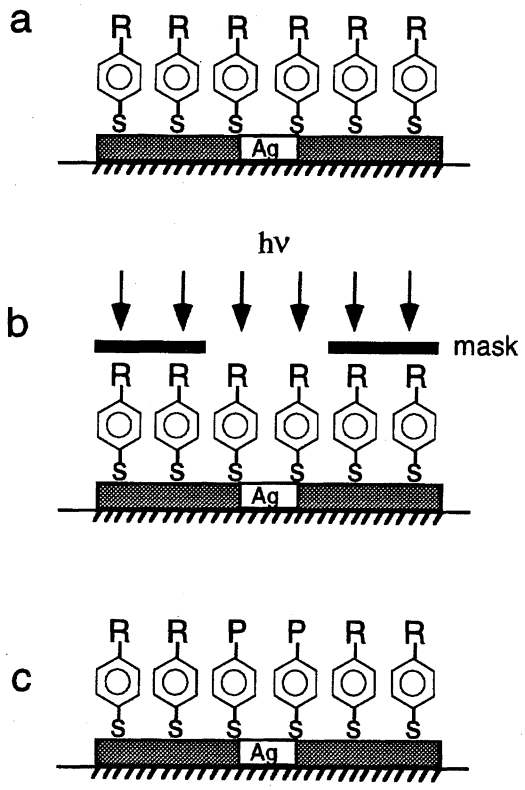

Fig. 3. Schematic diagram of the photopatterning of self-assembled molecular monolayers.

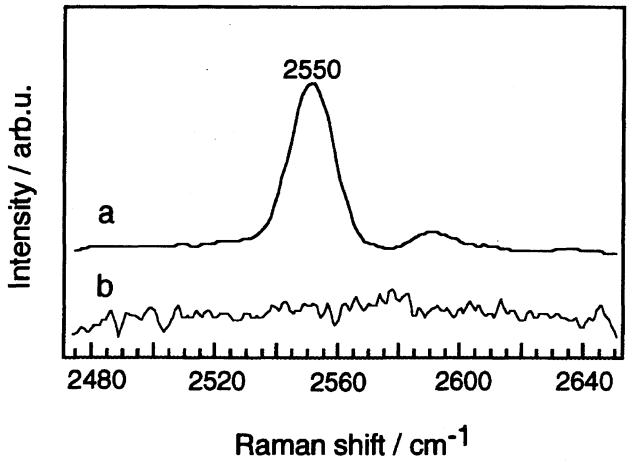

Fig. 4. SERS spectra for a) PNTP powder and b) PNTP SAM on silver in the S–H stretching region.

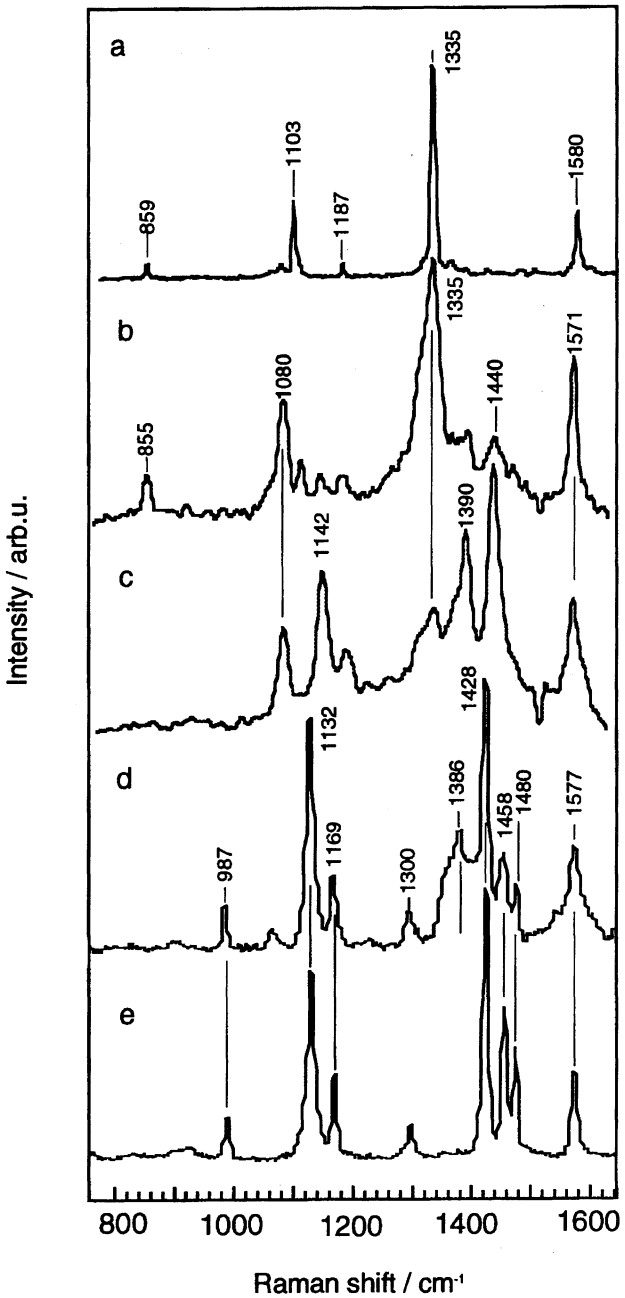

Fig. 5. SERS spectra: a) PNTP powder, b) PNTP SAM without UV illumination, c) PNTP SAM after 30 min UV illumination at 30 mW cm^{-2}, d) azobenzene adsorbed on evaporated Ag film, and e) azobenzene powder.

significantly different from the powder spectrum, as pointed out by Roth et al.[60] This phenomenon has been shown to be due to a laser-induced photochemical reaction (see Discussion below). During UV illumination, most of the original peaks lost intensity, and a new set of peaks appeared (Fig. 5, curve c). These new peaks rapidly increased in intensity, and the spectrum after 10 min was essentially identical to that after 30 min.

There is no clear consensus in the literature as to the assignment of the photoproduct peaks, including those at 1142, 1390, and 1440 cm^{-1}. Some authors ascribe similar spectral features, obtained via either electrochemical reduction of PNTP,[27,33] or to photochemical reduction,[34] to an aminobenzene-like species. Others ascribe such features, obtained during either photolysis[60–62] or electrolysis[61] of *p*-nitrobenzoic acid on silver, to the corresponding azobenzene-like species. A detailed study of this problem is beyond the scope of this paper and will be taken up in a separate publication.[50] However, in terms of the present work, it is important to try to understand whether the photoreaction is reversible or not, due to our interest in developing an erasable read-write system. If the photoproduct is *p*-aminothiophenol (PATP), the reaction should be reversible, i.e., it should be possible to

Table 1. Raman Peaks (cm^{-1}) and Assignments for *p*-Nitrothiophenol (PNTP) and Azobenzene (AB)

PNTP powder	PNTP SAM on Ag	Photolyzed PNTP SAM on Ag[a)]	AB adsorbed on Ag	AB powder	Mode	Comments	Reference
859	855				10a	CH wag	24,71
			987	987	12	Aromatic sextant stretch	71,72
1103	1080	1080			1	Aromatic whole ring stretch	24
		1142	1132	1132	C–N, 13/9a	Aromatic modes	72
			1169	1169	9b	Aromatic in-plane bending	72
			1300	1300	14	Aromatic in-plane bending	72
1335	1335	1335			N–O	NO_2 symmetric stretch	71,72
		1390	1386		N–N	N–N adsorbed on Ag	This work
	1440[b)]	1440	1428	1428	N–N	N–N, 19a/b mixed	72
			1458	1458	19b	Aromatic semicircle stretch	72
			1480	1480	19a	Aromatic semicircle stretch	72
1580	1571	1571	1577	1577	8a	Aromatic quadrant stretch	24, 71, 72

a) Exposed to UV illumination at 30 mW cm^{-2} for 30 min. b) Low intensity peak.

re-oxidize PATP back to PNTP. If, however, the product is the azobenzene derivative, the reaction would be much less reversible.[59] In Fig. 5, curves d and e, are shown a SERS spectrum for azobenzene, adsorbed on an evaporated silver film, and a powder spectrum for azobenzene, respectively. All of the peaks in the powder spectrum can be unequivocally assigned (Table 1). For azobenzene adsorbed on silver, there is an additional peak at 1390 cm^{-1}, which is most likely assignable to a perturbed N–N stretching mode. In the powder spectrum, this mode appears at 1428 cm^{-1}, but coordination of the N=N double bond directly with the silver surface, similar to the case with adsorption of C=C or C≡C groups on silver,[69] could lead to a substantial downward shift in frequency.

There is relatively good agreement between the spectrum for the photolyzed PNTP (Fig. 5, curve c) and that expected for a mixture of adsorbed PNTP and adsorbed azobenzene (Table 1), although the photolyzed PNTP spectrum does not exhibit peaks at ca. 855 or at ca. 988 cm^{-1}. Also, there is no evidence for the lower intensity peaks at ca. 1460 and ca. 1480 cm^{-1} that are found for azobenzene itself (see Fig. 5, curves d and e). The correspondence is sufficient, however, that it may reasonably be concluded that the photoproduct is an azobenzene-like species, and thus it may be difficult to re-oxidize it back to the PNTP form, either chemically or electrochemically.

It is interesting to note that, even in the non-photolyzed PNTP SAM, (Fig. 5, curve b), there is a small peak at 1440 cm^{-1}, which is most likely due to the N=N stretching mode of the azo group. The presence of this peak is understandable, because, during the image acquisition, the laser power density is relatively high at each 2 μm diameter spot (ca. 1.6×10^{3} W cm^{-2}), even though the time is short (0.6 s). During the UV photolysis procedure, the power density is much less (ca. 3×10^{-2} W cm^{-2}), although the time is long (ca. 2400 s). McGlashen et al. have pointed out the risk of laser-induced damage with focused beams at higher laser power levels, particularly with green laser light on roughened silver.[70]

Imaging of Photopatterned SAM. No matter what the precise nature of the photoreaction, however, several very definite points can be made. First, the spectrum for the photoproduct is clearly distinguishable from that for the parent compound, which allows us to clearly image the areas which have been illuminated. The peak at 1440 cm^{-1} is the most prominent one for the photoproduct, and it can be used to create a "positive" image, i.e., one in which bright areas in the image correspond to illuminated areas of the sample (Fig. 6b). The peak at 1335 cm^{-1} is the most prominent one for PNTP itself, and thus it can be used to produce a "negative" image, in which dark areas in the image correspond to illuminated areas of the sample (Fig. 6c). These peaks are relatively intense and have the least degree of interference from adjoining peaks. The dimensions of the pattern match closely the actual dimensions of the Cu grid used as a photomask (Fig. 6a). The contrast values that were obtained, defined as the ratio of counts measured in lighter vs. darker areas, were approximately 20 and 15, respectively, for Figs. 6b and 6c.

Microcontact Printing. The principle of microcontact printing is schematically depicted in Fig. 7. As noted by Whitesides and co-workers, a key to the success of this technique is the principle of "autophobicity," i.e., after the formation of the self-assembled monolayer, there is no tendency for the formation of multiple adsorbed layers.[9,12]

In the case of microcontact printing, evidence for the formation of an assembled PNTP monolayer on the silver surface was also found, i.e., the loss of the characteristic S–H stretching band at 2550 cm^{-1}.[23,24,26] The SERS spectrum for the assembled layer was essentially the same as that shown in Fig. 5 (curve b). Again, we selected the SERS peak at 1335 cm^{-1} as the most appropriate for the production of images since this peak is relatively intense and has relatively little interference from adjoining peaks.

Figure 8a shows an AFM image of the Cr mask used as the stamp in forming the patterned monolayer. A typical SERS image obtained from the PNTP-patterned silver surface is shown in Fig. 8b. The bright areas in Fig. 8b correspond

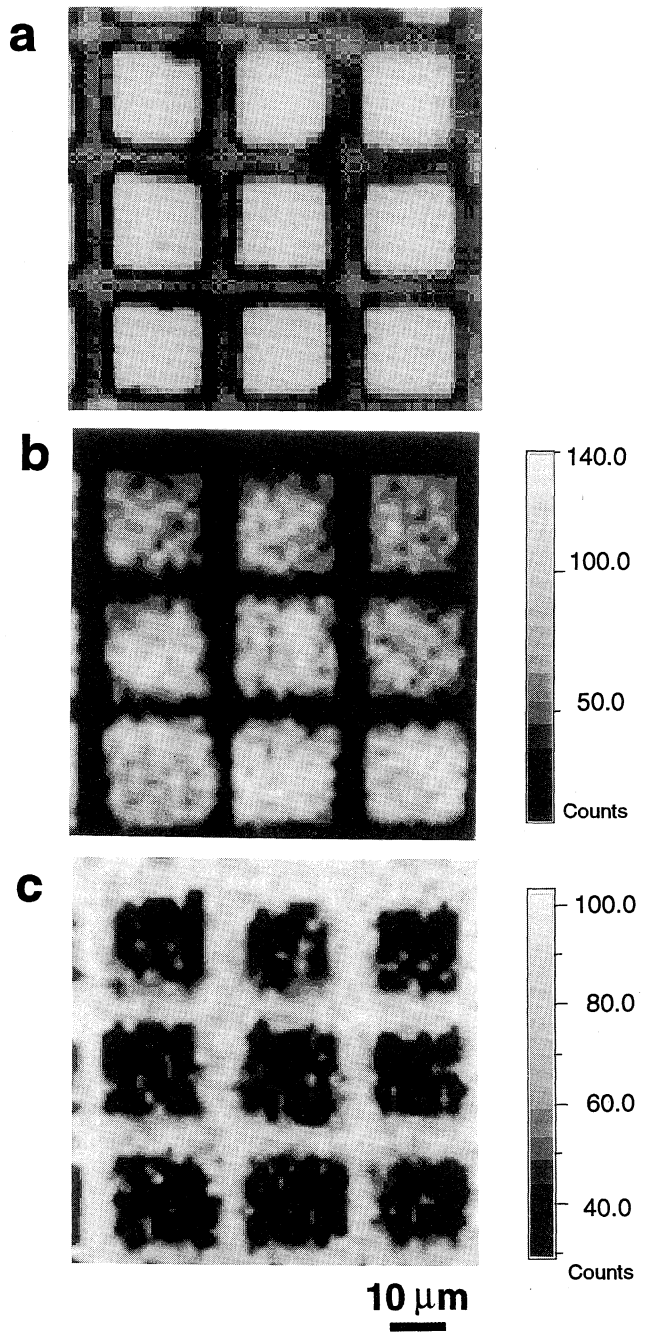

Fig. 6. SER images (80 μm×80 μm) obtained from a photopatterned (30 min., UV illumination at 30 mW cm^{-2}, using the Cu grid shown in part a) PNTP SAM on silver, corresponding to b) the 1440 cm^{-1} photoproduct peak and c) the 1335 cm^{-1} PNTP peak. Lighter areas are due to higher SERS intensity.

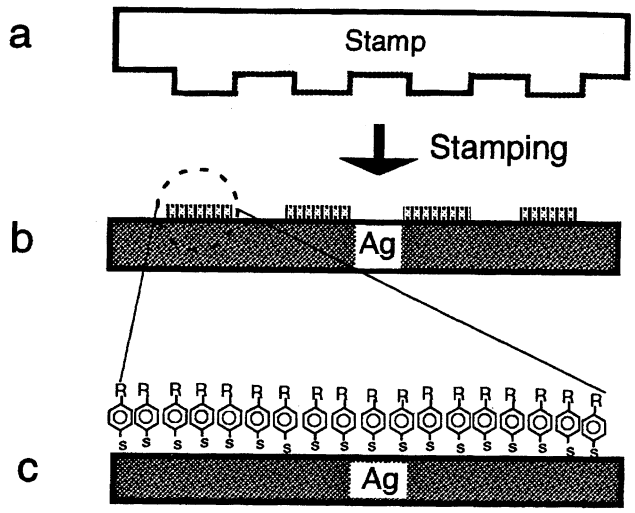

Fig. 7. Schematic diagram of the microcontact printing technique.

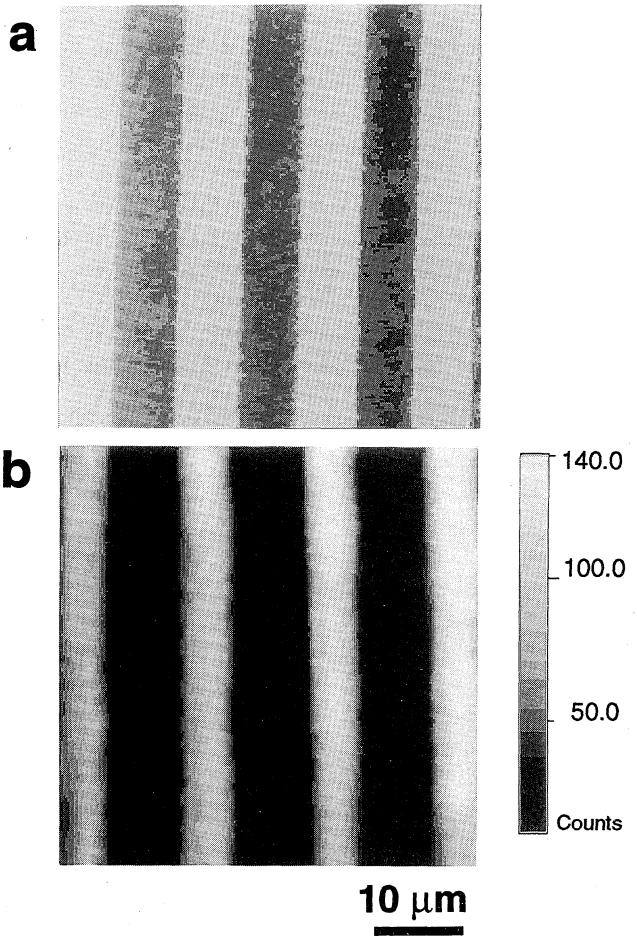

Fig. 8. Microcontact printing technique: a) AFM image of the stamp, and b) SER image corresponding to the 1335 cm^{-1} PNTP peak.

to high SERS intensity and are thus due to PNTP, while the dark regions correspond to low SERS intensity, due to the bare silver surface. The dimensions of the SERS-based image match closely those of the Cr strips in the stamp, although the former were slightly narrower than the latter. This is most likely due to the fact that the Cr strips are non-absorbent, and thus insufficient ink could be supplied to the evaporated silver surface. It should also be noted that AFM was used to examine the silver surface after assembly of the PNTP patterned monolayer, but no image of the pattern could be observed.

The average contrast, defined as the ratio of counts mea-

sured in lighter vs. darker areas, was approximately 20. The currently used acquisition time, yielding a total acquisition time of 40 min, would have to be considerably increased in order to improve the contrast noticeably. Images can also be obtained in a much shorter time, with a lower limit of on the order of 1 s, if a tunable filter is used in place of the monochromator and the CCD camera is used to obtain the two-dimensional spatial information in a direct imaging mode (see, for example, Refs. 37, 40, and 45). With conventional filters, there is usually poorer image quality compared to the point-by-point mode, but recently this problem has been alleviated through the use of acousto-optically tunable filters (AOTFs).[45]

In order to explore further the idea of chemical selectivity, the same approach was also followed with several other types of terminal groups. Thiophenols with COOH, OH, and CH_3 groups in the para position were examined. Resulting Raman spectra are shown in Fig. 9. Corresponding SER images are shown in Fig. 10. In this case, areas of the stamp were used with several different numbers of lines per mm. The image quality for the COOH and CH_3 terminal groups (Fig. 10, parts a and c) was quite high.

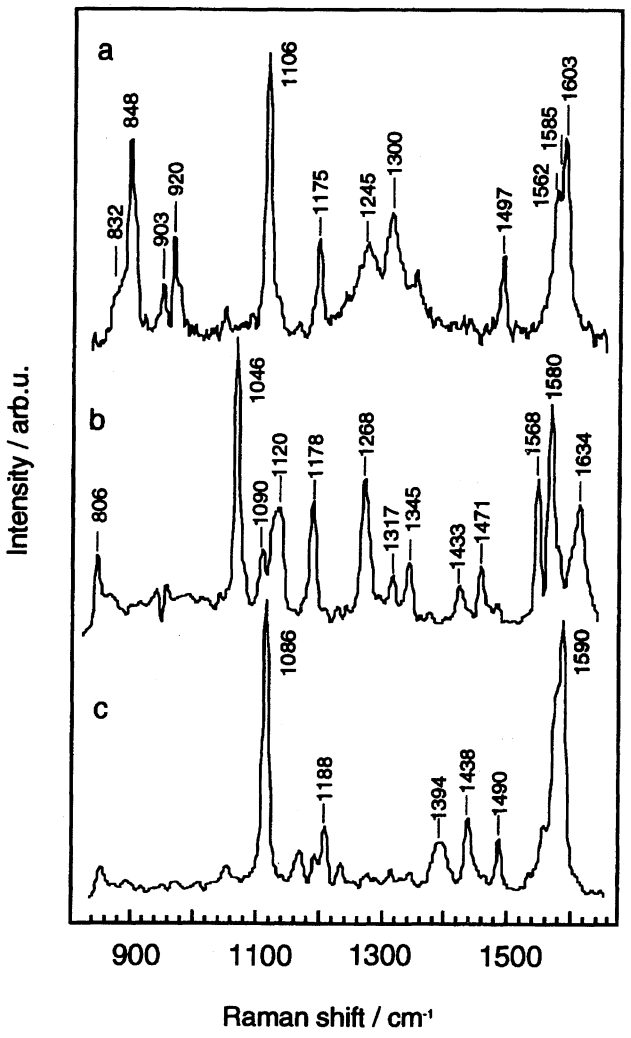

Fig. 9. SERS spectra for SAMs with various terminal functional groups: a) OH, b) COOH, and c) CH_3.

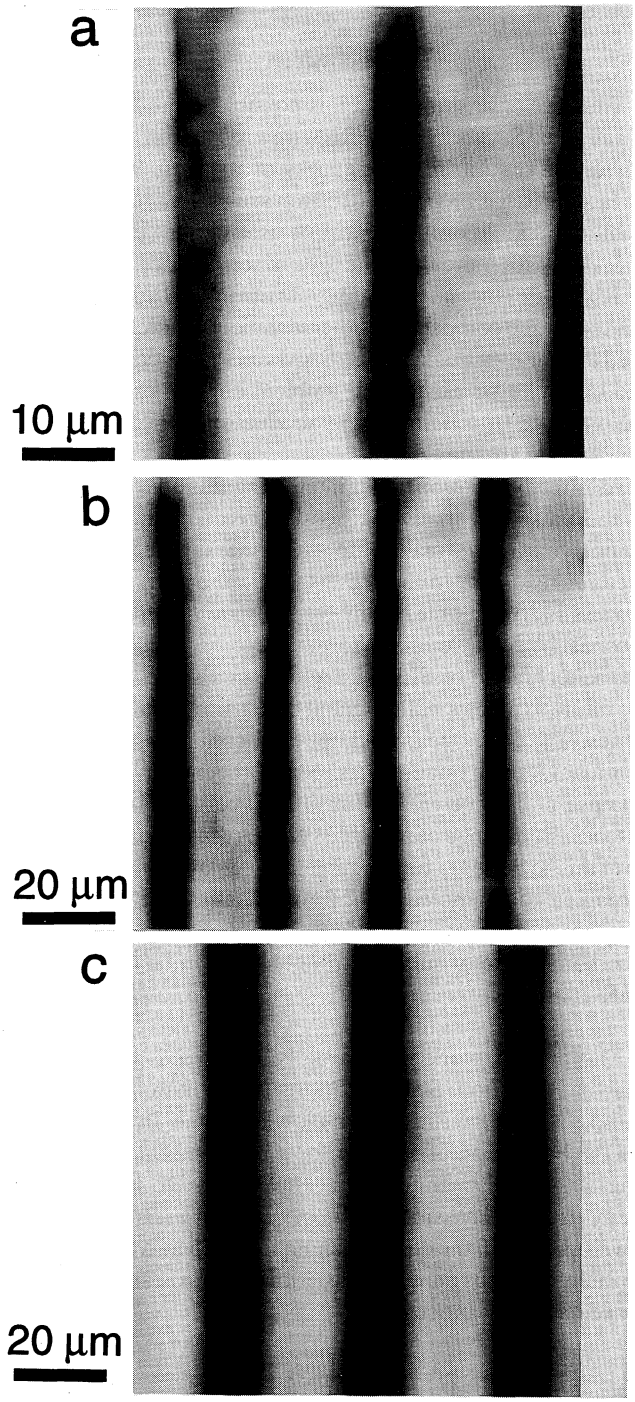

Fig. 10. SER images corresponding to the three types of SAMs in Fig. 9, with the frequencies of the Raman peaks used for imaging as follows: (a) 1106 cm^{-1}; (b) 1046 cm^{-1}; and (c) 1086 cm^{-1}.

Work is currently in progress to examine SAMs composed of two or more terminal groups. Comparison of the respective spectra shows that all of the possible pairs except for one should show reasonably good contrast. The exception is the COOH/CH_3 pair, as in both cases the most intense peaks happen to be located in the same spectral regions (Fig. 9,

parts b and c).

Conclusions

Thus, we have shown that it is possible to produce images of patterned SAMs using SERI, with a resolution of ca. 2 μm, relying on the intrinsic roughness of the evaporated silver surface, which is on the 50—100 nm scale. This new imaging technique should prove to be quite useful in the examination of SAMs with more than one type of termination, a prospect which we are currently pursuing. The principal advantages of this technique compared to other techniques which have been used to characterize patterned SAMs are chemical selectivity and ability to be used under ambient conditions or even in the presence of a liquid, as in an electrochemical cell with aqueous electrolyte.

As already mentioned, an interesting possible application of the present work is the possibility of using assembled monolayers as information storage devices, with SERS being used for read-out. In the present work, the image formation process is irreversible. However, we are also pursuing the prospect of erasable image formation.

The technique of SERS imaging can also be extended in the future to much smaller spatial dimensions using near-field optics. The use of near-field optics in conjunction with conventional Raman imaging has recently been demonstrated.[43] The use of surface enhancement may be quite important in extending the range of possible systems that can be examined with this technique, for example molecular monolayers and biological macromolecules. However, a limiting factor is the fact that, at current levels of sensitivity for Raman systems, a certain degree of substrate roughness is in fact needed for SER imaging.

The present work was partially supported by the Ministry of Education, Science, Sports and Culture. One of the authors (XMY) wishes to acknowledge the Japan Society for the Promotion of Science for a postdoctoral fellowship. The authors also gratefully acknowledge Dr. K. Ajito for many useful discussions and experimental assistance in the development of the SERI technique and Mr. M. Watanabe for helpful discussions and experimental assistance with the photopatterning process.

References

1) C. D. Frisbie, E. W. Wollman, J. R. Martin, and M. S. Wrighton, *J. Vac. Sci. Technol. A*, **11**, 2368 (1993).
2) M. J. Tarlov, J. D. R. F. Burgess, and G. Gillen, *J. Am. Chem. Soc.*, **115**, 5305 (1993).
3) E. W. Wollman, C. D. Frisbie, and M. S. Wrighton, *Langmuir*, **9**, 1517 (1993).
4) E. W. Wollman, D. Kang, C. D. Frisbie, I. M. Lorkovic, and M. S. Wrighton, *J. Am. Chem. Soc.*, **116**, 4395 (1994).
5) C. D. Frisbie, E. W. Wollman, and M. S. Wrighton, *Langmuir*, **11**, 2563 (1995).
6) C. S. Dulcey, J. J. H. Georger, V. Krauthamer, D. A. Stenger, T. L. Fare, and J. M. Calvert, *Science*, **252**, 551 (1991).
7) N. L. Abbott, J. P. Folkers, and G. M. Whitesides, *Science*, **257**, 1380 (1992).
8) G. P. Lopez, H. A. Biebuyck, C. D. Frisbie, and G. M. Whitesides, *Science*, **260**, 647 (1993).
9) H. A. Biebuyck and G. M. Whitesides, *Langmuir*, **10**, 2790 (1994).
10) A. Kumar and G. M. Whitesides, *Science*, **263**, 60 (1994).
11) M. O. Wolf and M. A. Fox, *J. Am. Chem. Soc.*, **117**, 1845 (1995).
12) A. Kumar, N. L. Abbott, E. Kim, H. A. Biebuyck, and G. M. Whitesides, *Acc. Chem. Res.*, **28**, 219 (1995).
13) C. S. Dulcey, J. J. H. Georger, M.-S. Chen, S. W. McElvany, C. E. O'Ferrall, V. I. Benezra, and J. M. Calvert, *Langmuir*, **12**, 1638 (1996).
14) L. F. Chi, R. R. Johnston, and H. Ringsdorf, *Langmuir*, **7**, 2323 (1991).
15) S. W. Hui, H. Yu, Z. Xu, and R. Bittman, *Langmuir*, **8**, 2724 (1992).
16) M. H. P. Moers, H. E. Gaub, and N. F. van Hulst, *Langmuir*, **10**, 2774 (1994).
17) R. M. Overney, E. Meyer, J. Frommer, D. Brodbeck, R. Luthi, L. Howald, H.-J. Guentherodt, M. Fujihira, H. Takano, and Y. Gotoh, *Nature*, **359**, 133 (1992).
18) C. D. Frisbie, L. F. Rozsnyai, A. Noy, M. S. Wrighton, and C. M. Lieber, *Science*, **265**, 2071 (1994).
19) S. Akari, D. Horn, H. Keller, and W. Schrepp, *Adv. Mater.*, **7**, 549 (1995).
20) J. L. Wilbur, H. A. Biebuyck, J. C. MacDonald, and G. M. Whitesides, *Langmuir*, **11**, 825 (1995).
21) G. P. Lopez, H. A. Biebuyck, and G. M. Whitesides, *Langmuir*, **9**, 1513 (1993).
22) A. Kumar, H. A. Biebuyck, and G. M. Whitesides, *Langmuir*, **10**, 1498 (1994).
23) T. H. Joo, K. Kim, and M. S. Kim, *J. Phys. Chem.*, **90**, 5816 (1986).
24) T. H. Joo, S. Kim, and K. Kim, *J. Raman Spectrosc.*, **18**, 57 (1987).
25) M. A. Bryant and J. E. Pemberton, *J. Am. Chem. Soc.*, **113**, 8284 (1991).
26) M. A. Bryant and J. E. Pemberton, *J. Am. Chem. Soc.*, **113**, 3629 (1991).
27) N. Matsuda, K. Yoshii, K. Ataka, M. Osawa, T. Matsue, and I. Uchida, *Chem. Lett.*, **1992**, 1385.
28) T. Sueoka, J. Inukai, and M. Ito, *J. Electron Spectrosc. Rel. Phenom.*, **64/65**, 363 (1993).
29) W. B. Caldwell, K. Chen, B. R. Herr, C. A. Mirkin, J. C. Hulteen, and R. P. Van Duyne, *Langmuir*, **10**, 4109 (1994).
30) S. D. Evans, T. L. Freeman, T. M. Flynn, and D. N. Batchelder, *Thin Solid Films*, **244**, 778 (1994).
31) M. Osawa, N. Matsuda, K. Yoshii, and I. Uchida, *J. Phys. Chem.*, **98**, 12702 (1994).
32) W. B. Caldwell, D. J. Campbell, K. Chen, B. R. Herr, C. A. Mirkin, A. Malik, M. K. Durbin, P. Dutta, and D. G. Huang, *J. Am. Chem. Soc.*, **117**, 6071 (1995).
33) M. Futamata, *J. Phys. Chem.*, **99**, 11901 (1995).
34) N. Matsuda, T. Sawaguchi, M. Osawa, and I. Uchida, *Chem. Lett.*, **1995**, 145.
35) D. J. Campbell, B. R. Herr, J. C. Hulteen, R. P. VanDuyne, and C. A. Mirkin, *J. Am. Chem. Soc.*, **118**, 10211 (1996).
36) T. Xiao, Q. Ye, and L. Sun, *J. Phys. Chem. B*, **101**, 632 (1997).
37) P. J. Treado and M. D. Morris, *Appl. Spectrosc.*, **44**, 1 (1990).
38) R. V. Sudiwala, C. Cheng, E. G. Wilson, and D. N.

Batchelder, *Thin Solid Films*, **210/211**, 452 (1992).
39) A. Fujishima, L. A. Nagahara, H. Yoshiki, K. Ajito, and K. Hashimoto, *Electrochim. Acta*, **39**, 1229 (1993).
40) G. J. Puppels, M. Grond, and J. Greve, *Appl. Spectrosc.*, **47**, 1256 (1993).
41) K. Ajito, J. P. H. Sukamto, L. A. Nagahara, K. Hashimoto, and A. Fujishima, *J. Electroanal. Chem.*, **386**, 229 (1995).
42) K. Ajito, J. P. H. Sukamto, L. A. Nagahara, K. Hashimoto, and A. Fujishima, *J. Vac. Sci. Technol. A*, **13**, 1234 (1995).
43) C. L. Jahncke, M. A. Paesler, and H. D. Hallen, *Appl. Phys. Lett.*, **67**, 2483 (1995).
44) C. L. Jahncke, H. D. Hallen, and M. A. Paesler, *J. Raman Spectrosc.*, **27**, 579 (1996).
45) H. R. Morris, C. C. Hoyt, P. Miller, and P. J. Treado, *Appl. Spectrosc.*, **50**, 805 (1996).
46) C. M. Stellman, K. S. Booksh, and M. L. Myrick, *Appl. Spectrosc.*, **50**, 552 (1996).
47) X. M. Yang, K. Ajito, D. A. Tryk, K. Hashimoto, and A. Fujishima, *J. Phys. Chem.*, **100**, 7923 (1996).
48) X. M. Yang, D. A. Tryk, K. Ajito, K. Hashimoto, and A. Fujishima, *Langmuir*, **12**, 5525 (1996).
49) X. M. Yang, D. A. Tryk, K. Hashimoto, and A. Fujishima, *Appl. Phys. Lett.*, **69**, 4020 (1996).
50) X. M. Yang, D. A. Tryk, K. Hashimoto, and A. Fujishima, manuscript in preparation, (1997).
51) X. M. Yang, M. Noguchi, D. A. Tryk, K. Hashimoto, and A. Fujishima, manuscript in preparation, (1997).
52) B. Pettinger and U. Wenning, *Chem. Phys. Lett.*, **56**, 253 (1978).
53) B. Pettinger, U. Wenning, and D. M. Kolb, *Ber. Bunsenges. Phys. Chem.*, **82**, 1326 (1978).
54) S. G. Schultz, M. Janik-Czachor, and R. P. Van Duyne, *Surface Sci.*, **104**, 419 (1981).
55) Y. Mo, I. Moerke, and P. Wachter, *Surface Sci.*, **133**, L452 (1983).
56) V. L. Schlegel and T. M. Cotton, *Anal. Chem.*, **63**, 241 (1991).
57) R. P. Van Duyne, J. C. Hulteen, and D. A. Treichel, *J. Chem. Phys.*, **99**, 2101 (1993).
58) J. A. Barltrop and N. J. Bunce, *J. Chem. Soc.*, **1968**, 1467.
59) A. P. Tomilov, S. G. Mairanovskii, M. Y. Fioshin, and V. A. Smirnov, "Electrochemistry of Organic Compounds," Halstead Press, New York (1972), p. 248.
60) P. G. Roth, R. S. Venkatachalam, and F. J. Boerio, *J. Chem. Phys.*, **85**, 1150 (1986).
61) S. Sun, R. L. Birke, J. R. Lombardi, K. P. Leung, and A. Z. Genack, *J. Phys. Chem.*, **92**, 5965 (1988).
62) H. Bercegol and F. J. Boerio, *J. Phys. Chem.*, **99**, 8763 (1995).
63) A. Kumar and G. M. Whitesides, *Appl. Phys. Lett.*, **63**, 2002 (1993).
64) A. Kumar, H. A. Biebuyck, and G. M. Whitesides, *Langmuir*, **10**, 1498 (1994).
65) R. Singhvi, A. Kumar, G. P. Lopez, G. N. Stephanopoulos, D. I. C. Wang, G. M. Whitesides, and D. E. Ingber, *Science*, **264**, 696 (1994).
66) J. L. Wilbur, A. Kumar, E. Kim, and G. M. Whitesides, *Adv. Mater.*, **6**, 600 (1994).
67) F. J. Garcia-Vidale and J. B. Pendry, *Phys. Rev. Lett.*, **77**, 1163 (1996).
68) J. Huang, D. A. Dahlgren, and J. C. Hemminger, *Langmuir*, **10**, 626 (1994).
69) M. L. Patterson and M. J. Weaver, *J. Phys. Chem.*, **89**, 5046 (1985).
70) M. L. McGlashen, U. Guhathakurta, K. L. Davis, and M. D. Morris, *Appl. Spectrosc.*, **45**, 543 (1991).
71) N. B. Colthup, L. H. Daly, and S. E. Wiberley, "Introduction to Infrared and Raman Spectroscopy," 3rd ed, Academic Press, Boston (1990).
72) D. R. Armstrong, J. Clarkson, and W. E. Smith, *J. Phys. Chem.*, **99**, 17825 (1995).